Direct and Inverse Resonance Problems for Shielded Composite Objects Treated by Means of the Null-Field Method

WENXIN ZHENG

Abstract—**Resonances of a composite object shielded by a perfect conductor are investigated using the null-field method. Computed resonance frequencies and quality factors of shielded homogeneous and composite resonators are reported and compared with previously published results whenever possible. Conversely, in the inverse sense, the permittivities and geometric parameters of shielded composite objects are computed from calculated or measured complex frequencies.**

I. Introduction

THE RESONANCE frequencies and the quality factors of various modes of an open composite object, such as a dielectric/ferrite ring or a double dielectric disk, can be computed accurately by means of the null-field method [1]. However, in an actual microwave circuit, a dielectric resonator is rarely used without a metallic housing to obtain a higher Q factor and reduce its radiation interference. In the present paper, a study of metallic shielded composite objects by means of the null-field method is reported.

The electromagnetic resonances of a metallic shielded dielectric object with a specific geometry have been studied by many authors. For instance, a dielectric sphere shielded by a concentric metallic sphere has been analyzed using a rigorous analysis method [2]. One or several dielectric cylindrical rods or rings shielded by a coaxial cylindrical housing have been investigated using various mode-matching techniques [3]–[5]. A surface integral technique based on the method of moments [6] has been used to evaluate a shielded dielectric resonator. The merits and shortcomings of most of these methods are described and compared in [3].

The null-field method has been used to study a variety of exterior problems (see e.g. [1] and references given therein). It has also been applied to several interior problems, such as the resonances in electromagnetic absorption by lossy dielectric objects [7], the transmission and reflection of waves by an obstacle inside a waveguide [8], and passbands and stopbands for a waveguide with arbitrary cross section [9] or with a corrugated wall [10]. In this paper, the null-field formulation for shielded objects is derived in Section II. Computed resonance frequencies of shielded objects and Q factors for lossy materials are reported in Section III and compared with other published results whenever possible. In Section IV, the method is used to solve the corresponding inverse problem, e.g., to find the complex permittivities, permeabilities, and/or geometric parameters from known (measured) resonance frequencies and Q factors. Section V gives some general concluding remarks.

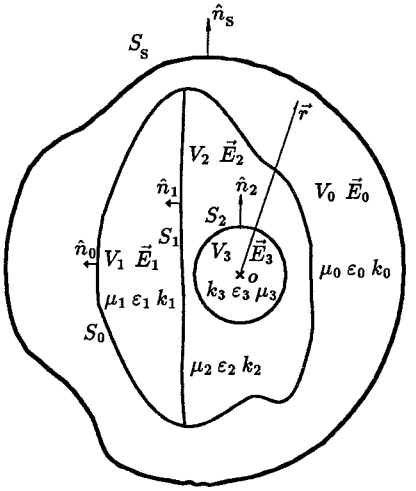

Fig. 1. Geometry and notations of a metallic shielded composite permeable object consisting of three homogeneous parts.

II. Formulation

We consider the general case of a shielded object consisting of a perfectly conducting shield enclosing a composite object. The composite object could consist of a number of obstacles as described in [11], could comprise several homogeneous parts forming a chainlike structure as discussed in [12] and [13], or could comprise layerlike inhomogeneities as in [1] and [14] (an example of a shielded object with three homogeneous parts is given in Fig. 1). We assume that an origin O can be chosen inside the composite object and that a finite sum of the vector spherical waves or vector spherical harmonics defined with respect to this origin can be used to approximate the unknown surface fields. We also assume that the annular

Manuscript received January 4, 1989; revised June 1, 1989.

The author is with the Department of Electromagnetic Theory, Royal Institute of Technology, S-100 44 Stockholm, Sweden.

IEEE Log Number 8930669.

0018-9480/89/1100-1732$01.00 ©1989 IEEE

region between the shield and the object, denoted by V_0, is filled with a homogeneous material, and that the electromagnetic properties of the homogeneous material in each region V_j, where $j=0,1,\cdots,M$ (we assume that the composite object has M homogeneous parts), can be described by a scalar relative permittivity ϵ_j and a scalar relative permeability μ_j. The wavenumber k_j in V_j can then be expressed in terms of a frequency f_0 as $k_j=k_0\sqrt{\epsilon_j\mu_j}=2\pi f_0\sqrt{\epsilon_j\mu_j}/c$, where c is the speed of light in vacuum. If the losses due to a nonvanishing conductivity and the damping caused by the alternating polarization of the material in the region V_j are considered, the permittivity can be expressed by a complex value in the form

$$\epsilon_j=\epsilon_j'+i\frac{\sigma_j}{2\pi f_0}$$

and the loss tangent can be defined as the ratio of the imaginary part to the real part of ϵ_j: $\tan\delta_j=\sigma_j/(2\pi f_0\epsilon_j')$, where σ_j is the equivalent conductivity causing all the losses in the material in the region V_j. The time factor is $e^{-i\omega t}$.

In the following we denote the inner surface of the shield by S_s, a bounding surface of the whole composite object by S_0, and the outward unit normal on the surfaces by $\hat{n}$ with a corresponding subscript. We assume that S_s and S_0 are disjoint, but we do not rule out cases where points on S_0 can approach points on S_s as close as we please. The electric field in V_0 is denoted by $\vec{E}_0$.

We assume that the sources are located in the annular region V_0. Let R_s denote the radius of a circumscribed sphere of S_s, with its center at O. Similarly, let r_0 denote the radius of an inscribed sphere of S_0, with center at O. Thus, the incident field $\vec{E}^{\text{in}}$ excited by the sources can be expanded in terms of regular spherical waves, $\operatorname{Re}\vec{\psi}_n(k\vec{r})$, inside the sphere with the radius r_0, and in terms of outgoing spherical waves, $\vec{\psi}_n(k\vec{r})$, outside the sphere with the radius R_s, respectively, as follows:

$$\vec{E}^{\text{in}}(\vec{r})=\sum_n a_n\operatorname{Re}\vec{\psi}_n(k_0\vec{r}),\qquad |\vec{r}|<r_0 \tag{1}$$

$$\vec{E}^{\text{in}}(\vec{r})=\sum_n b_n\vec{\psi}_n(k_0\vec{r}),\qquad |\vec{r}|>R_s. \tag{2}$$

The definitions of the regular and outgoing spherical waves can be found in [1]. An abbreviated multi-index notation $n\equiv(\tau,\sigma,m,l)$ with

$$\tau=1,2\qquad \sigma=e,o\ (\text{"even" or "odd"})$$
$$m=0,1,\cdots,l\qquad l=1,2,\cdots$$

has been used (cf. [1]). The expansion (1) is valid inside any sphere with center at O which does not contain any of the sources of $\vec{E}^{\text{in}}$. The expansion (2) is valid outside any sphere with center at O which encloses all of the sources of $\vec{E}^{\text{in}}$. We apply the null part of Green's second theorem twice to the region V_0 by first considering $|\vec{r}|<r_0$ and then $|\vec{r}|>R_s$, respectively. Thus two equations are obtained on the bounding surfaces of the annular region, S_0 and S_s, in the form

$$a_n=-ik_0\int_{S_s-S_0}\left[\nabla'\times\vec{\psi}_n(k_0\vec{r}')\cdot(\hat{n}\times\vec{E}_0)+\vec{\psi}_n(k_0\vec{r}')\cdot\left(\hat{n}\times(\nabla'\times\vec{E}_0)\right)\right]dS' \tag{3}$$

$$b_n=-ik_0\int_{S_s-S_0}\left[\nabla'\times\operatorname{Re}\vec{\psi}_n(k_0\vec{r}')\cdot(\hat{n}\times\vec{E}_0)+\operatorname{Re}\vec{\psi}_n(k_0\vec{r}')\cdot\left(\hat{n}\times(\nabla'\times\vec{E}_0)\right)\right]dS'. \tag{4}$$

The boundary condition for the electric field on the perfectly conducting surface S_s is

$$\hat{n}_s\times\vec{E}_0(\vec{r}')=0,\qquad \vec{r}'\text{ on }S_s. \tag{5}$$

We can approximate the magnetic surface field on S_s by using a series of regular spherical waves and a set of unknown coefficients $\{\alpha_n\}$ [15] as follows:

$$\hat{n}_s\times\left(\nabla\times\vec{E}_0(\vec{r}')\right)=\sum_{n'}^{N}\alpha_{n'}\left[\hat{n}_s\times\left(\nabla\times\operatorname{Re}\vec{\psi}(k_0\vec{r}')\right)\right]. \tag{6}$$

Different procedures for obtaining the matrices which characterize the composite object bounded by S_0 can be adopted for the different geometric structures mentioned in the beginning of this section. Independent of the procedure that is used, after introducing the boundary conditions and expanding the surface fields (cf., e.g., [11]–[15]), one always arrives at the matrix equations (with $\vec{a}\equiv\{a_n\}$, $\boldsymbol{Q}=\{Q_{nn'}\}$, etc.) of the following form:

$$\vec{a}=i\left[\boldsymbol{Q}_S(\vec{\psi})\vec{\alpha}-\boldsymbol{Q}_R(\vec{\psi})\vec{\beta}\right] \tag{7}$$

$$\vec{b}=i\left[\boldsymbol{Q}_S(\operatorname{Re}\vec{\psi})\vec{\alpha}-\boldsymbol{Q}_R(\operatorname{Re}\vec{\psi})\vec{\beta}\right] \tag{8}$$

where the elements of $\boldsymbol{Q}_S$ are defined by

$$\left[\boldsymbol{Q}_S(\vec{\Psi})\right]_{nn'}=k_0\int_{S_s}\vec{\Psi}_n(k_0\vec{r}')\times\left[\nabla'\times\operatorname{Re}\vec{\psi}_{n'}(k_0\vec{r}')\right]\cdot\hat{n}_s\,dS'. \tag{9}$$

However, the form of the $\boldsymbol{Q}_R$ matrices for the composite dielectric/ferrite resonator and the meaning of the set of the unknown coefficients, $\vec{\beta}$, depend on the particular null-field approach used for the composite object bounded by S_0. The procedure suggested in [1] has been found flexible and suitable to most of the resonance problems treated in this paper. The sequence of truncations that will be considered on the right-hand side of (6), and in the following matrix relations, is determined by a sequence of values $l_{\max}$, where for each $l_{\max}$ one considers all $l\leqslant l_{\max}$; $m=0,1,\cdots,l$; $\tau=1,2$; and $\sigma=e,o$. For a given $l_{\max}$ the number of terms on the right-hand side of (6) is $N=2(l_{\max}+2)\times l_{\max}$.

Since the resonances of a linear system correspond to the eigensolutions of the related homogeneous system, i.e., the solution of the linear equations without any excitation, (7) and (8) can be used to solve the resonance problem by setting $\vec{a}=0$ and $\vec{b}=0$. After obvious calculation, one finds that, in order to have nontrivial solutions, the determinant of the following matrix representation must vanish,

namely,

$$\det\left\{\boldsymbol{Q}_S(\mathrm{Re}\,\vec{\psi})\left[\boldsymbol{Q}_S(\vec{\psi})\right]^{-1}\boldsymbol{Q}_R(\vec{\psi})-\boldsymbol{Q}_R(\mathrm{Re}\,\vec{\psi})\right\}=0. \tag{10}$$

We remember that the zeros of $\det[\boldsymbol{Q}_S(\mathrm{Re}\,\vec{\psi})]$ represent the resonances of the empty metallic cavity (cf., e.g., [16]), while zeros of $\det[\boldsymbol{Q}_R(\vec{\psi})]$ represent the resonances of the open composite object (cf. [1]). From (10) it is seen that the resonances of the shielded object will in general be different from the resonances of the shield and of the object itself, respectively. Therefore, we can rewrite (10) and search for the zeros of the shielded object according to the following equation:

$$\det(\boldsymbol{R})\equiv\det[\boldsymbol{T}_S-\boldsymbol{T}_R]=0 \tag{11}$$

where $\boldsymbol{T}_S=-\boldsymbol{Q}_S(\mathrm{Re}\,\vec{\psi})[\boldsymbol{Q}_S(\vec{\psi})]^{-1}$ is the transition matrix of the corresponding perfectly conducting shield, while $\boldsymbol{T}_R=-\boldsymbol{Q}_R(\mathrm{Re}\,\vec{\psi})[\boldsymbol{Q}_R(\vec{\psi})]^{-1}$ is the transition matrix of the corresponding open composite object (cf., e.g., [15]). We should mention here that (11) is only written for the analysis below, while (10) should be used to calculate the zeros; this is because the zeros of (11) comprise a subset of the zeros of (10). The sets differ by the intersection of the zeros of $\det[\boldsymbol{Q}_R(\vec{\psi})]=0$ and the zeros of (10). However, so far we have never encountered any point in the intersection in our numerical calculations. Because the transition matrices, $\boldsymbol{T}_S$ and $\boldsymbol{T}_R$, are symmetric complex matrices [15], the $N\times N$ matrix $\boldsymbol{R}$ is symmetric and thus it can always be diagonalized by a unitary matrix $\boldsymbol{U}$ in the form $\boldsymbol{R}=\boldsymbol{U}\Lambda\boldsymbol{U}^T$ [17], where $\boldsymbol{U}^T$ is the transpose of $\boldsymbol{U}$, and Λ is a real nonnegative diagonal matrix, $\Lambda\equiv\mathrm{diag}(\lambda_1,\lambda_2,\cdots,\lambda_N)$. Thus a zero of (11) must satisfy at least one of the following system of equations of the singular values of the R matrix:

$$\lambda_i(k_0)=0,\qquad i=1,2,\cdots,N.$$

The form of this equation depends on the electromagnetic parameters and geometric shape of the resonator. Let $\{P\}$ denote a set of electromagnetic parameters ϵ_j', μ_j, and σ_j, $j=0,1,\cdots,M$. Similarly, one often considers, e.g., a specified class of geometric objects, which can be characterized by a set of geometrical parameters $\{G\}$ (with its elements consisting of the length and radius of a pillbox, two half-axes of an ellipsoid, etc.). For such a situation we may indicate the dependence of λ_i on $\{G\}$ and $\{P\}$ explicitly as follows:

$$\lambda_i(\{k_0\};\{G\},\{P\})=0,\qquad i=1,2,\cdots,N. \tag{12}$$

We note that each equation in the system (12) has an infinite number of roots, and that each root in each equation represents a particular resonant mode. We also note that these roots are, in general, complex numbers, although the singular values, λ_i, $i=1,2,\cdots,N$, are all real.

In the direct problem, the sets $\{G\}$ and $\{P\}$ are known and one searches for a set of roots of (12), $\{k_0\}$, in the complex plane, i.e., the resonance frequencies and the quality factors (for lossy materials). Alternatively, one can also use the same equations and the same procedures to solve an inverse problem within, e.g., specified classes of geometries from measured natural frequencies; i.e., from a set of known $\{k_0\}$ one searches for a finite set of unknowns in $\{G\}$ and/or $\{P\}$ using a suitable optimization method. Of course, the solution is not unique since there are infinitely many roots to the equations. But in many situations, the "desired" root can be distinguished using prior knowledge when the number of the unknowns is not too large. The numerical method employed in this paper to find the roots for both direct and inverse problems is the secant method. Some numerical examples of direct and inverse problems are given in Sections III and IV, respectively.

III. Numerical Results for Direct Problems

For general three-dimensional shielded objects, the Q and T matrices obtained in the previous section are full matrices. However, for some special geometries simplifications occur. As discussed in [1], the Q matrices for an axisymmetric shielded object have only diagonal blocks (with $m=m'$) different from zero, which correspond to different azimuthal dependences of the resonant fields. Furthermore, for a concentric layered dielectric sphere with a concentric spherical shield, choosing the geometric center as the origin, one obtains diagonal matrices which have explicit analytic expressions for the diagonal elements of the T_S [11] and T_R [18] matrices. In practice, all the computations are repeated with increasing matrix size (corresponding to increasing consecutive $l_{\max}$ values) until a specific convergence requirement is met. However, for the case of a layered concentric spherical structure, the zeros of (10) or (12) do not depend upon the matrix size.

To verify the method developed in the preceding section, the resonance frequencies and the Q factors are computed and compared with published results [2] for a lossy spherical dielectric resonator shielded by a concentric sphere (SSS). The loss tangent of the material is $\tan\delta=f_0/40000$. The curves shown in Fig. 2 are all calculated using two positions of the origin, $d=0$ and $d=a/2$, respectively, where d is the distance between the geometric center and the origin chosen. When the off-center origin is used the matrices are no longer diagonal and the zeros depend on the matrix size. Comparison of the results obtained for a $d=0$ and a $d\neq 0$ case provides a check on the computer codes. The results for $d=0$ and $d=a/2$ agree for at least the first five digits (i.e., on the scale of Fig. 2 the results overlap completely). In the present paper, we always assume that the shield is a perfect conductor. Thus, only the dielectric quality factors, Q_d, are reported in the results of this paper. From Fig. 2 and [2] one can see that the Q_d dominates the unloaded Q factor when the resonance frequency of a certain mode is close to that of the corresponding open resonator (flatter parts of the curves of the resonance frequencies, as shown in Fig. 2(a)). In the layered concentric spherical structure, there exist only transverse electric (TE) and transverse magnetic (TM) modes. Three subscripts, *mlp*, have been used to distinguish the

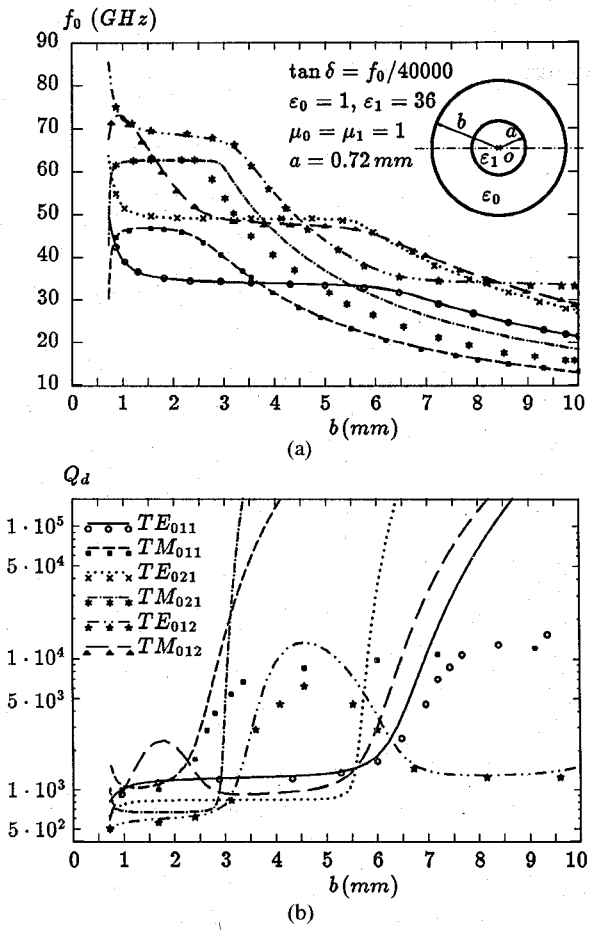

Fig. 2. Mode chart of lossy dielectric sphere shielded by a concentric metallic sphere (SSS). The various lines are computed using the present method for perfectly conducting shield while markers represent results reported in [2], in which loss of the shield has been taken into account. (a) Resonance frequencies. (b) Quality factors.

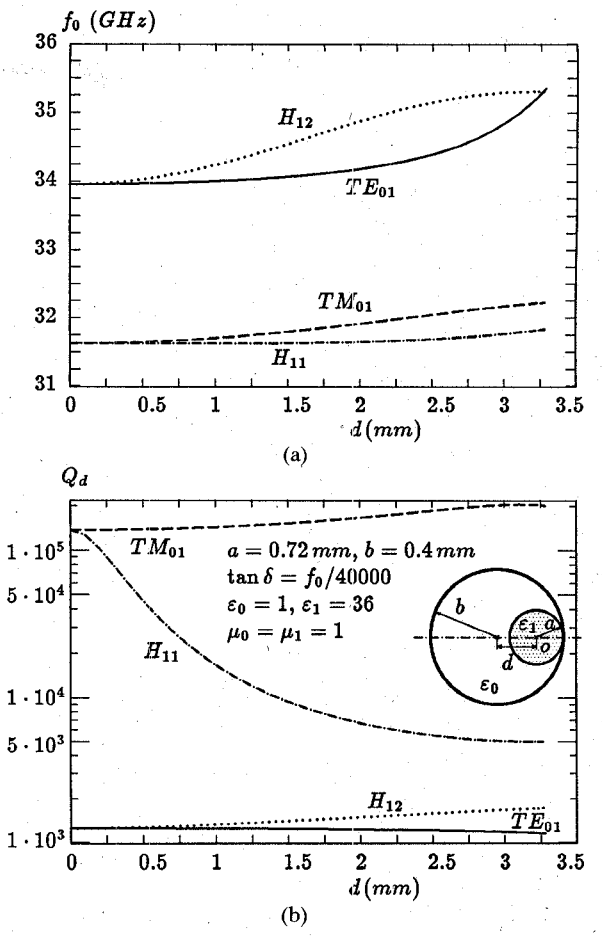

Fig. 3. Mode chart of a lossy dielectric sphere shielded by an eccentric perfectly conducting metallic sphere. (a) Resonance frequencies. (b) Quality factors.

modes in the same class, where m and l appeared above in the multi-index n, while p refers to the pth root. For this spherical structure both the present method and that of [2] can be regarded as exact methods. Very good agreement is found except for the TM_{021} mode. As for the TM_{021} mode, we have confidence in our results since the resonance frequency of this mode at $b = 10$ mm from our calculation ($f_0 = 18.47869$) is much closer to that of the empty metallic cavity (the exact value for the empty cavity is $f_0 = 18.47903$; cf., e.g., [19]).

For a slightly more complicated geometry, such as the eccentric spherical resonator and shield in Fig. 3 and most of the following examples, the rigorous and numerical methods based on standard separation-of-variables techniques can no longer be applied. The resonance properties of an eccentrically mounted resonator which has the same geometry and electromagnetic properties as that in Fig. 2 are illustrated in Fig. 3. Besides the TE and TM modes observed in Fig. 2, the hybrid electromagnetic modes (H modes) appear when $d > 0$. In this and following examples without a concentric SSS structure, we use two subscripts, ml, to designate the different modes in the same class. The first index, m, refers to the azimuthal dependence of the modes of axisymmetric bodies and the second, l, is the order of the resonance frequency, $l = 1$ being the lowest resonance of the particular mode. This mode designation scheme originates from [20] with a slight simplification (since the object considered in Fig. 3 does not have the symmetry plane perpendicular with the symmetry axis, which was used in [20]).

In Fig. 4, the resonance frequencies and Q_d values are plotted and compared for three different concentric geometries, i.e., sphere-shielded sphere (SSS), sphere-shielded pillbox (SSP), and pillbox-shielded sphere (PSS). From this figure one observes very similar effects for the three different structures. There is at least one flatter part ("plateau") in every curve depicted in Fig. 4(a). In this part, the frequency remains essentially independent of the size of the shield and is very close to the resonance frequency of the corresponding mode of the open resonator. The Q_d factor can be approximated by $1/\tan\delta$ and it is much smaller than the quality factors of ordinary metallic cavities. On the two sides of the plateau, the resonance frequency and the quality factor variations follow those of the dielectric-filled (left) and the empty (right) metallic cavity, respectively, for the corresponding mode, as have been observed for a cylinder-shielded pillbox [3] and a SSS [2]. In Fig. 4 one can also find that the TE_{01} and H_{11}

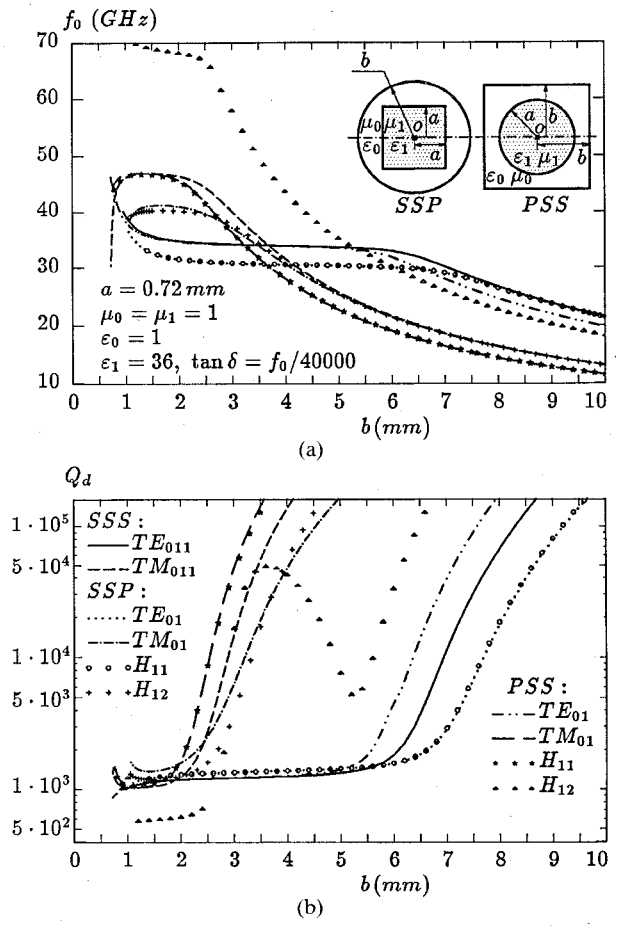

Fig. 4. Comparison of the resonance frequencies and quality factors of different modes between a sphere-shielded sphere (SSS), a sphere-shielded pillbox (SSP), and a pillbox-shielded sphere (PSS). (a) Resonance frequencies. (b) Quality factors.

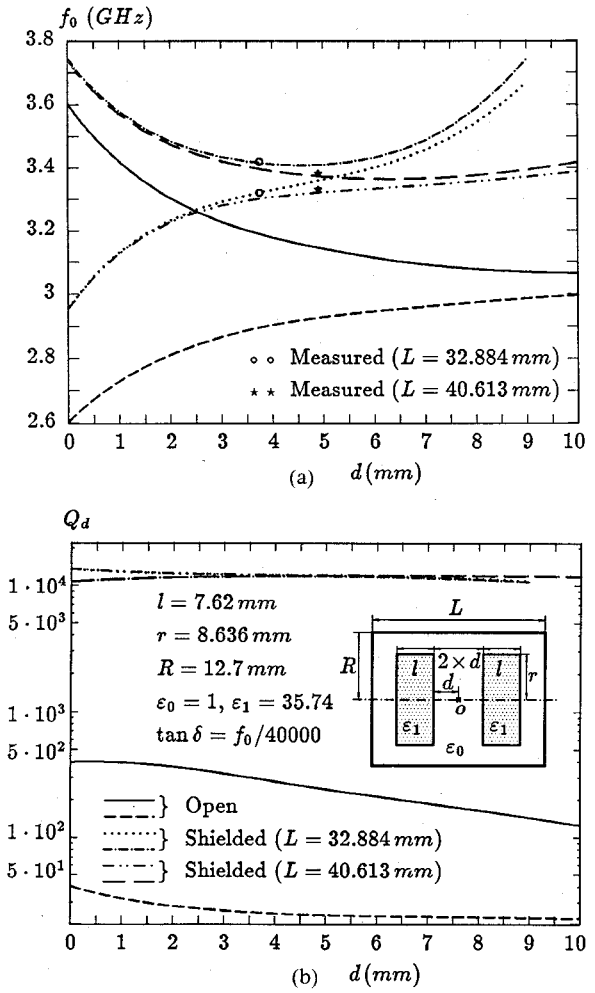

Fig. 5. Comparison of the resonance frequencies and the quality factors of two of the TE modes between an open and two shielded lossy dielectric double disks. The measured values are reported in [4]. (a) Resonance frequencies. (b) Quality factors.

modes of the SSP and the TM_{01} and H_{11} modes of the PSS degenerate to one another, respectively, for almost the entire range of the radius, b, of the shield. This is related to the fact that special pillboxes (length equal to diameter) are used in the two cases; it is not a general feature.

The composite object inside the shield need not be permeable; it can contain one or several conducting parts (cf. [11]–[15]). As an example, we consider the somewhat unusual shielded object provided by the earth itself with the ionosphere as the shield. We model the earth by a perfectly conducting spheroid of equatorial radius 6378 km and polar radius 6356 km. The ionosphere is modeled by a concentric perfectly conducting spherical shield of radius 6500 km. The first eight resonance frequencies computed using the null-field method are $f_0 = 10.83$ (TM_{01}), 18.31 (TM_{02}), 20.54 (TE_{01}), 25.80 (TM_{03}), 29.01 (TE_{02}), 33.26 (TM_{04}), 37.28 (TE_{03}), and 40.70 (TM_{05}) Hz. The zeros of the hybrid modes deviate very little from those of the TE and TM modes. The shift is within 2 percent, because the object is almost a sphere. From the observation of the peaks in a typical noise power spectrum recorded at Lavangsdalen, these Schumann resonances (cf. [21]) have average linear frequencies of 8, 14, 20.2, 25.7, 28.3, 32.5, 34, 37.3, and 41.7 Hz, respectively. The lack of precise agreement, especially for the first two peaks, is not surprising, since the assumption of perfectly conducting walls is very crude. However, the $\sqrt{l(l+1)}$ variation of the computed resonance frequencies for each of the TE and TM modes is quite striking.

A set of double dielectric pillbox structures, one open case and two shielded cases with different sizes of the shield, are considered and the resonance frequencies and Q factors of the two lowest TE modes of each case are computed and plotted in Fig. 5. Some measured results from [4] have also been included in Fig. 5 for comparison. The lower and the upper TE mode correspond to the $TE_{01\delta}$ and the $TE_{01\delta+1}$ mode, respectively, of a single pillbox resonator (cf. [1]) for each case. The larger the separation of the two pillboxes, the closer the resonance frequencies of the two TE modes; thus the smaller the coupling coefficient (cf., e.g., [4]) between the two resonators. For the open case, the resonance frequencies of the two TE modes approach the same limit as d increases, namely the resonance frequency of the $TE_{01\delta}$ mode of a single pillbox resonator. On the other hand, for the shielded cases, the resonance frequencies increase again when the pillboxes

TABLE I
DIRECT AND INVERSE RESONANCE RESULTS FOR THE TE_{011} MODE OF A SPHERICAL RESONATOR CONCENTRICALLY SHIELDED BY A METALLIC SPHERE AS SHOWN IN FIG. 2

Known Data of the TE_{011} Mode						Reconstructed Data	
a (mm)	b (mm)	ε_1	f_0 (GHz)	Q_d	Errors	Computed Results	Errors
0.72	4.0	36+i0.03056	—	—	—	f_0=33.958298, Q_d=1256.18	—
—	4.0	36+i0.03056	33.96	1260	0.005%	a=0.71996	0.005 %
—	4.0	36+i0.03056	34.3	1270	1%	a=0.7126	1 %
0.72	—	36+i0.03056	33.96	1260	0.005%	b=3.993	0.18 %
0.72	—	36+i0.03056	34.3	1270	1%	b=2.798	30 %
0.72	4.0	—	33.96	1260	0.005%	ε_1=35.996+i0.03047	0.03 %
0.72	4.0	—	34.3	1270	1%	ε_1=35.239+i0.02965	3 %

TABLE II
DIRECT AND INVERSE RESONANCE RESULTS FOR THE TM_{011} MODE OF A SPHERICAL RESONATOR CONCENTRICALLY SHIELDED BY A METALLIC SPHERE AS SHOWN IN FIG. 2

Known Data of the TM_{011} Mode						Reconstructed Data	
a (mm)	b (mm)	ε_1	f_0 (GHz)	Q_d	Errors	Computed Results	Errors
0.72	4.0	36+i0.02847	—	—	—	f_0=31.631401, Q_d=137014.	—
—	4.0	36+i0.02847	31.63	137000	0.005%	a=0.72030	0.005 %
—	4.0	36+i0.02847	32	140000	1%	a=0.6314	12.3 %
0.72	—	36+i0.02847	31.63	137000	0.005%	b=4.0002	0.005 %
0.72	—	36+i0.02847	32	140000	1%	b=3.948	1.3 %
0.72	4.0	—	31.63	137000	0.005%	ε_1=36.346+i0.02866	0.95 %
0.72	4.0	—	31.6	140000	1%	ε_1=44.161+i0.02994	22 %

approach the ends of the shield and then form new pillboxes with double thickness together with their mirror images in the perfectly conducting plane walls of the shield.

IV. Results for Inverse Problems

From (12) one can see that every object, open or shielded, has its intrinsic complex resonance frequencies, known as the natural frequencies, in the electromagnetic spectrum, and that the location of these frequencies in the complex plane depends upon $\{G\}$ and $\{P\}$, i.e., its size, shape, and internal structure. The identification of the object (including its shield, if any) by the natural frequencies is one of the branches in the area of the inverse problem which has been the subject of intense research. Some practical applications have been carried out in this branch, such as the measurement of dielectric properties of low-loss materials [22], the determination of the moisture content in single soybean seeds [23], and accurately sizing the diameter of glass fiber [18]. The application of equations (10)–(12) to the inverse problems can be classified as the singularity expansion method (cf. [24]–[26]) in the frequency domain. Since there are many methods available for accurate measurement of the resonance frequencies and corresponding Q values of shielded or open composite objects (cf., e.g., [3] and its references) or, alternatively, for extraction of the natural frequencies from the transient scattered signal in the time domain (cf., e.g., [27]), we only give examples of using the known complex frequencies to determine the physical characteristics of the objects.

We first consider the simplest case, a concentric SSS as shown in Fig. 2. From those computed complex resonance frequencies, we can reconstruct radii of the resonator, a, and shield, b, the complex permittivity of the resonator, ϵ_1, etc., within any prescribed accuracy. However, no such "clean" data can be obtained in any actual measurements. The errors in the results reconstructed from measured data can be estimated by a factor

$$F_p = \frac{k_0}{p}\cdot\frac{\partial p}{\partial k_0} \approx \frac{k_0}{p}\cdot\frac{\Delta p}{\Delta k_0}, \qquad p \in \{G\}\cup\{P\}. \quad (13)$$

If F_p is found to be much bigger than unity, the computed result is often not reliable since the errors from the measurement have been magnified. Thus, it is important to choose a set of suitable modes for a concrete problem from which a relatively smaller F_p can be achieved. In Tables I and II, reconstructed data for a concentric SSS are listed for different parameters using the TE_{011} and the TM_{011} mode, respectively. From these tables one observes that the TE_{011} mode is not very appropriate for the reconstruction of b at $b = 4$ mm ($F_{b=4} \approx 34$), while TM_{011} ($F_{b=4} \approx 1$) works very well (cf. also Fig. 2). A similar situation (sometimes TE_{011} becomes a favorite mode) occurs when one wants to reconstruct other parameters, such as a and ϵ_1, for a known b.

A similar procedure can also be applied to an inverse problem for an open object, for which the zeros are searched for with $\det\{Q_R\}$ (cf. [1]) instead of (10). Taking an open dielectric pillbox ($r = 5.25$ mm, $L = 4.6$ mm) as an example, we list the computed permittivities in Table III by using the measured resonance frequencies and Q values due to radiation for four different modes reported by Kajfez *et al.* [28]. The relative permittivity, ϵ_1, of the material used is assumed to be 38. The average relative

TABLE III
COMPUTED PERMITTIVITIES, ϵ_1, OF AN OPEN DIELECTRIC PILLBOX WITH RADIUS $r = 5.25$ MM, LENGTH $L = 4.6$ MM, AND $\mu_1 = 1$ FROM MEASURED RESONANCE FREQUENCIES AND Q VALUES DUE TO RADIATION

Measured Data [28]			Computed Results	
modes	f_0 (GHz)	Q	ϵ_1	Errors
$TE_{01\delta}$	4.85	51	38.178	0.47%
$TM_{01\delta}$	7.60	86	37.340	-1.74%
$HEM_{12\delta}$	6.64	64	38.246	0.65%
$HEM_{21\delta}$	7.81	204	37.533	-1.23%
Average	—	—	37.824	-0.46%

The know ϵ_1 of the material is 38.

error with respect to $\epsilon_1 = 38$ is 0.46 percent, which is very close to the typical accuracy of measurement of the dielectric constant (0.3 percent [3]), although the errors in the measurement of the resonance frequencies and Q's have not yet been taken into account.

As a last example, we consider a peanutlike layered dielectric object with a dry shell ($\epsilon_1 = 9$) and a wet prolate spheroidal core shielded by a concentrically placed cylindrical metallic cavity, as illustrated in Fig. 6. The permittivity of the core, ϵ_2, can be expressed by a linear function of the water content, c ($0 \leqslant c \leqslant 1$), in the core (cf., e.g., [29]):

$$\epsilon_2 = \epsilon_{\text{dry}} + (\epsilon_{\text{water}} - \epsilon_{\text{dry}}) \cdot c \tag{14}$$

where the permittivity of the dry core is chosen the same as the shell (i.e., $\epsilon_{\text{dry}} = \epsilon_1$) and the dielectric constant of water is $\epsilon_{\text{water}} \approx 79 + i25$ [29]. The resonance frequencies and Q_d factors of the lowest TE mode were first computed for various water contents, $c = 0 \sim 20$ percent, to obtain "clean data." To imitate the measured resonance frequencies and Q values, two different levels of uniformly distributed pseudorandom noise, corresponding to relative errors of 1 percent and 5 percent, respectively, were added to the real and imaginary parts of the complex clean data. From the corrupted data, the complex permittivities and the corresponding water content of the core were reconstructed. The reconstructed points in Fig. 6(a) are all on the top of the curve of the clean data, as expected, since the linear relation (14) has been used. The reconstructions, shown in Fig. 6, are only an illustration of the possibilities of the present method. For more realistic problems (determination of the water content in a single seed, melting hailstone, etc.), more accurate models of the relation between the water content and the permittivity and more appropriate resonant modes have to be used.

V. CONCLUDING REMARKS

In the present article an approach within the general framework of the null-field method to the direct and inverse resonance problems of shielded composite objects is suggested, and implemented numerically for axially symmetric structures. Good convergence and reasonable agreement with other computed and measured results are achieved for both direct and inverse resonance problems.

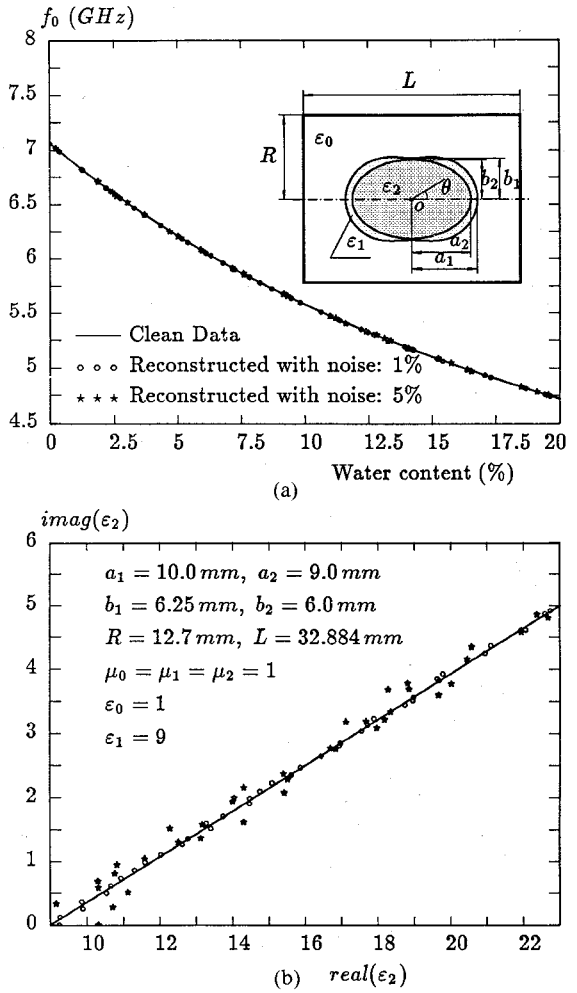

Fig. 6. Clean and reconstructed data of a cylinder-shielded lossy peanutlike object. The lossless shell of the object is bounded internally by a spheroid and externally by the surface with a contour satisfying $r(\theta) = (a_1^2 \cos^2\theta + b_1^2 \sin^2\theta)^{1/2}$, respectively. (a) Resonance frequencies. (b) Permittivities.

Finally, we remark that in applications of the null-field approach a basic criterion is that of stability of the results (concerning, typically, surface-field expansion coefficients, inverses of Q matrices, T matrix elements, zeros of $\det[Q]$, etc.) as the truncation order (determined by $l_{\max}$) is increased (cf., e.g., [1], [12]–[15]). Thus, the dependence of the choice of $l_{\max}$ for all the quantities studied in the present paper has been investigated and has, in all the examples presented, been found to satisfy predetermined limitations. Illustrations of the typical convergence behavior for similar problems can be found in [1, table I].

ACKNOWLEDGMENT

The author would like to thank Prof. S. Ström for his encouraging and valuable advice in the present work and Dr. G. Kristensson for his helpful comments on this paper.

REFERENCES

[1] W. Zheng, "Computation of complex resonance frequencies of isolated composite objects," *IEEE Trans. Microwave Theory*, vol. 37, pp. 953–961, June 1989.
[2] A. Julien and P. Guillon, "Electromagnetic analysis of spherical dielectric shielded resonators," *IEEE Trans. Microwave Theory Tech.*, vol. MTT-34, pp. 723–729, June 1986.

[3] D. Kajfez and P. Guillon, Eds., *Dielectric Resonators*. Norwood, MA: Artech House, 1986.
[4] K. A. Zaki and C. Chen, "Coupling of non-axially symmetric hybrid modes in dielectric resonators," *IEEE Trans. Microwave Theory Tech.*, vol. MTT-35, pp. 1136–1142, Dec. 1987.
[5] Y. Kobayashi and M. Minegishi, "Precise design of a bandpass filter using high-Q dielectric ring resonators," *IEEE Trans. Microwave Theory Tech.*, vol. MTT-35, pp. 1156–1160, Dec. 1987.
[6] D. Kajfez and J. Lebaric, "Field patterns of TM_0 modes in a shielded dielectric resonator," *Electron. Lett.*, vol. 23, no. 18, pp. 944–946, Aug. 1987.
[7] P. W. Barber, "Resonance electromagnetic absorption by nonspherical dielectric object," *IEEE Trans. Microwave Theory Tech.*, vol. MTT-25, pp. 373–381, May 1977.
[8] A. Boström and P. Olsson, "Transmission and reflection of electromagnetic waves by an obstacle inside a waveguide," *J. Appl. Phys.*, vol. 52, no. 3, pp. 1187–1196, Mar. 1981.
[9] F. L. Ng and R. H. T. Bates, "Null-field method for waveguides of arbitrary cross section," *IEEE Trans. Microwave Theory Tech.*, vol. MTT-20, pp. 658–662, Oct. 1972.
[10] S. L. G. Lundqvist, "Electromagnetic waves in a cylindrical waveguide with infinite or semi-infinite wall corrugations," *IEEE Trans. Microwave Theory Tech.*, vol. 36, pp. 28–33, Jan. 1988.
[11] Bo Peterson and S. Ström, "T-matrix for electromagnetic scattering from an arbitrary number of scatterers and representations of E(3)," *Phys. Rev. D*, vol. 8, pp. 2670–2684, 1974.
[12] S. Ström and W. Zheng, "The null-field approach to electromagnetic scattering from composite objects," *IEEE Trans. Antennas. Propagat.*, vol. 36, pp. 376–382, Mar. 1988.
[13] W. Zheng, "The null-field approach to electromagnetic scattering from composite objects: The case with three or more constituents," *IEEE Trans. Antennas Propagat.* vol. 36, pp. 1396–1400, Oct. 1988.
[14] W. Zheng and S. Ström, "The null-field approach to scattering from composite objects: The case of concavo-convex constituents," *IEEE Trans. Antennas Propagat.*, vol. 37, pp. 373–383, Mar. 1989.
[15] P. C. Waterman, "Symmetry, unitarity, and geometry in electromagnetic scattering," *Phys. Rev. D*, vol. 3, no. 4, pp. 825–839, 1971.
[16] G. Kristensson, "Natural frequencies of circular disks," *IEEE Trans. Antennas Propagat.*, vol. AP-32, pp. 442–448, May 1984.
[17] R. A. Horn and C. A. Johnson, *Matrix Analysis*. Cambridge, England: Press Syndicate of the University of Cambridge, 1985, ch. 4.
[18] P. W. Barber, J. F. Owen, and R. K. Chang, "Resonant scattering for characterization of axisymmetric dielectric objects," *IEEE Trans. Antennas Propagat.*, vol. AP-30, pp. 168–172, Mar. 1982.
[19] J. A. Kong, *Electromagnetic Wave Theory*. New York: Wiley, 1986, pp. 187–191.
[20] K. A. Zaki and C. Chen, "New results in dielectric-loaded resonators," *IEEE Trans. Microwave Theory Tech.*, vol. MTT-34, pp. 815–824, July 1986.
[21] J. D. Jackson, *Classical Electrodynamics*, 2nd ed. New York: Wiley, 1975, pp. 360–364.
[22] Y. Kobayashi and M. Katoh, "Microwave measurement of dielectric properties of low-loss materials by the dielectric rod resonator method," *IEEE Trans. Microwave Theory Tech.*, vol. MTT-33, pp. 586–592, July 1985.
[23] A. W. Kraszewski, T. S. You, and S. O. Nelson, "Microwave resonator technique for moisture content determination in single soybean seeds," in *Proc. 18th European Microwave Conf.*, (Stockholm), Sept. 1988, pp. 903–908.
[24] C. E. Baum, "The singularity expansion method," in *Transient Electromagnetic Fields*, L. B. Felsen, Ed. Heidelberg, Springer-Verlag, 1976.
[25] A. G. Tijhuis, *Electromagnetic Inverse Profiling*. Utrecht, VNU Science Press, 1987.
[26] L. W. Pearson, "A note on the representation of scattered fields as a singularity expansion," *IEEE Trans. Antennas Propagat.*, vol. AP-32, pp. 520–524, May 1984.
[27] M. A. Morgan, "Singularity expansion representations of fields and currents in transient scattering," *IEEE Trans. Antennas Propagat.*, vol. AP-32, pp. 466–473, May 1984.
[28] D. Kajfez, A. W. Glisson, and J. James, "Computed modal field distributions for isolated dielectric resonators," *IEEE Trans. Microwave Theory Tech.*, vol. MTT-32, pp. 1609–1616, Dec. 1984.
[29] K. Aydin, T. A. Seliga, and V. N. Bringi, "Differential radar scattering properties of model hail and mixed-phase hydrometeors," *Radio Sci.*, vol. 19, no. 1, pp. 58–66, Jan. 1984.

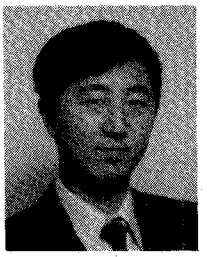

Wenxin Zheng was born in Beijing, China, in 1953. He received the M.S. degree in electrical engineering from the Graduate School of North China Institute of Electric Power in 1982. He is currently pursuing the Ph.D. degree in the Department of Electromagnetic Theory at the Royal Institute of Technology in Stockholm, Sweden.

Since 1984 he has held the position of Lecturer in the graduate school of North China Institute of Electric Power. His primary field of interest concerns computer solutions of electromagnetic field analysis problems. He has done research on applying finite element and finite difference methods to guided wave problems. He is currently engaged in the application of numerical methods to direct and inverse scattering and resonance problems for composite objects.